XLVI CILAMCE
VITÓRIA - ES - BRAZIL - 2025
XLVI IBERO-LATIN AMERICAN CONGRESS ON COMPUTATIONAL METHODS IN ENGENEERING

Multi-objective structural optimization of shallow domes considering geometric nonlinearity and grouping of bars

João Marcos de Paula Vieira[1], Afonso Celso de Castro Lemonge[1], Patrícia Habib Hallak[1], Érica da Costa Reis Carvalho[2], Dênis Emanuel da Costa Vargas[3]

[1]*Graduate Program in Computational Modeling, Federal University of Juiz de Fora*
Rua José Lourenço Kelmer, s/n, Campus Universitário Bairro São Pedro, 36036-900, Juiz de Fora, MG, Brasil
joaomarcos.vieira@estudante.ufjf.br, afonso.lemonge@ufjf.br, patricia.hallak@ufjf.br
[2]*Department of Computer Science, Federal University of São João del-Rei*
Av. Visc. do Rio Preto, s/n, Fábricas, 36301-360, São João del-Rei, MG, Brasil
ericacarvalho@ufsj.edu.br
[3]*Department of Mathematics, Federal Center for Technological Education of Minas Gerais*
Avenida Amazonas, 5253, Nova Suíça, 30421-169, Belo Horizonte, MG, Brasil
denis.vargas@cefetmg.br

Abstract. The formulation and solution of structural optimization problems in trusses is broadly discussed in the literature, commonly involving objective functions such as minimizing the structure's weight and nodal displacements. In most of these works, the structures present elastic and geometrically linear behavior. In this paper, a multi-objective structural optimization problem (MOSOP) is proposed, involving objective functions such as minimizing the weight of the structure, maximizing the first natural frequency of vibration, maximizing the critical load factor related to the global stability, and minimizing the number of distinct cross-sectional areas of the bars. The constraints are related to the maximum nodal displacements. The analyzed structure is a shallow truss dome with geometric nonlinearity. Therefore, a geometrically nonlinear analysis is performed to determine the deformed configuration of the structure with greater accuracy, using the cylindrical arc-length method. Three evolutionary algorithms are applied to solve the MOSOP, and the Pareto front obtained in the proposed problem is presented, illustrating, for example, how the growth of the dome's weight leads to increases in the first natural frequency of vibration. It is also possible to note how the grouping and arrangement of the bars can influence the values of the other objective functions. Finally, optimized solutions are extracted from the Pareto front based on the decision-maker's preferences.

Keywords: Multi-objective structural optimization, Geometrically nonlinear analysis, Shallow dome trusses.

1 Introduction

Structural optimization problems are often applied in the literature and in real-world projects to find structural configurations that satisfy the requirements imposed by a standard or a usually recommended practice. The most frequently used objective function is the minimization of the structure's weight, aiming to reduce the material consumption and construction costs. The literature also widely discusses problems with two or more conflicting objective functions, known as multi-objective structural optimization problems (MOSOPs). In most of these works, the structures present elastic and geometrically linear behavior. This paper proposes and solves a MOSOP with four objective functions. In addition to minimizing the weight, the other objective functions are related to the safety and usability of the structure (maximizing the first natural frequency of vibration and the first critical load factor regarding global stability), and also the organization and efficiency of the construction process (minimizing the number of different cross-sectional areas for the bars). The constraints are the maximum nodal displacements. The structure under study is a 60-bar truss dome, with the cross-sectional area of these bars as the sizing design variables. A geometrically nonlinear analysis is performed to define the displacements and deformed configurations of the truss, using the cylindrical arc-length method. Despite the higher computational costs, this analysis allows the decision-maker (DM) to obtain more realistic and accurate values regarding the objective functions and constraints, given the shallow dome's geometric nonlinearity.

Three differential evolution based algorithms are used to solve the proposed MOSOP, and the results are presented through Pareto fronts and parallel coordinate graphs. Afterwards, a multi-criteria decision-making (MCM) is applied to extract the desired solutions from the Pareto front (PF), according to the DM's preferences. Therefore, the main objective of this paper is to solve the MOSOP with the proposed objective functions and constraints, considering the geometric nonlinearity of the analyzed truss and extracting solutions according to the designer's criteria. The performances of the meta-heuristics in solving the optimization problem are also evaluated. This paper is organized as follows: Section 2 describes the aspects of the MOSOP and the algorithms covered in the paper. Section 3 discusses the concepts and the application of the geometrically nonlinear analysis. The analyzed structure and the MOSOP's formulation are presented in Section 4. Section 5 contains the results and analysis of the MOSOP, including the Pareto front and the non-dominated solutions extracted from it. Finally, the conclusions and future steps of this research are reported in Section 6.

2 Multi-objective structural optimization

This section contains a theoretical presentation of important concepts covered in this paper, such as the multi-objective structural optimization and the differential evolution algorithms adopted to solve the proposed problem. It also presents the structural importance of the objective functions applied in the MOSOP, the constraints of the problem, and the method applied to extract the desired solutions.

2.1 Definition, objective functions and constraints

By definition, MOSOPs present two or more objective functions to be minimized or maximized simultaneously. These objectives can be conflicting. The MOSOP proposed in this paper has four objective functions: the minimization of the structure's weight, the maximization of the first natural frequency of vibration, the maximization of the first critical load factor related to the global stability, and the minimization of the number of different cross-sectional areas for the groups of bars. The constraints are related to the maximum displacement allowed for the central node, and the boundaries of the search space. As commonly adopted in the literature, the first objective function is to minimize the weight, aiming to reduce the material consumption in the structure's design for economic, environmental, and structural reasons. As usual in the literature (e.g, in [1], [2], [3] and [4]), the total weight of the truss is approximated by the sum of each bar's weight, disregarding the masses of the connections and the non-structural masses acting on some of the nodes.

The resonance can be defined as the effect in which the frequency of the applied load equals a natural frequency of vibration of the structural system. As the structure operates near resonance, its displacements, vibrations, and accelerations intensify, shortening the structure's lifespan and potentially causing user discomfort, material fatigue, corrosion, and even collapse. To avoid these undesirable effects, the second objective function is to maximize the structure's first natural frequency of vibration, increasing its distance from the frequencies generated by the applied loads. The global stability of structures indicates their sensitivity to second-order effects, that is, those generated by their displacements. Therefore, verifying the global stability is an important requirement in the design of a structure, aiming to guarantee safety in terms of the ultimate limit state of stability. In this sense, the third objective function is the maximization of the first critical load factor, aiming to find solutions that allow the application of the highest possible load to the structure without causing instability. It is essential to note that in this paper, the critical load factor for the global stability was evaluated by solving a generalized eigenvalue problem that accounts for the structure in its final deflected form. This objective function directly impacts the maximization of the critical load at the point of loss of stability on the structure's load-displacement curve. Increasing the critical load factor increases the critical load at the point of instability. As detailed in Section 4, the analyzed dome is formed by 60 bars divided into 7 groups. Each group includes bars with the same cross-sectional area. In order to simplify the processes of purchasing materials, manufacturing, assembling, checking, welding, etc., the fourth objective function aims to minimize the number of bar groups with different cross-sectional areas. This value varies from 1 (all bars have the same section) to 7 (each group of bars presents a different cross-sectional area).

2.2 Algorithms and multi-criteria decision-making

One of the most popular meta-heuristics for solving optimization problems is the differential evolution algorithm (DE). Introduced by Storn and Price [5], it is based on the generation and evolution of a population of candidate solutions with continuous variables. Based on previous works in the literature [2, 4], three DE-based multi-objective structural optimization algorithms (MOEAs) are applied to solve the MOSOP proposed in this pa-

per: the success history–based adaptive multi-objective differential evolution (SHAMODE) and its variation using whale optimization (SHAMODE-WO), both proposed by Panagant *et al.* [6], in addition to the multi-objective meta-heuristic with iterative parameter distribution estimation (MM-IPDE), proposed by Wansasueb *et al.* [7]. Constraint-handling utilized either the constraint-based non-dominated sorting technique [8] or constraint dominance principles. Under these principles: (i) feasible solutions are prioritized over infeasible ones; (ii) among infeasible solutions, those with smaller constraint violations are ranked higher; and (iii) among feasible solutions, dominance determines the ranking. In the computational experiments conducted here, the algorithms were configured according to the parameters specified in their original references.

The non-dominated solutions provided by the MOEAs are presented through Pareto fronts and parallel coordinate graphs. To extract the desired solutions from the Pareto front, the multi-criteria tournament decision (MTD) method, proposed by Parreiras and Vasconcelos [9], is employed. Derived from the MCDM framework, this method ranks the best and worst solutions based on the values of the objective functions and the weights (w_i, given that $\sum_{i=1}^{N_{of}} w_i = 1$, and N_{of} is the number of objective functions) assigned to them by the decision-maker, according to the level of importance the DM attributes to each objective of the problem. A more detailed explanation of this operation can be found in [2, 9, 10]. Three distinct scenarios are proposed for the extraction of solutions with the MTD method: sc_1 with equal weights (w_{1-4} = 0.25) for all objective functions; sc_2 with the weight w_1 = 0.5 to minimize the dome's mass, while the other objective functions have equal weights among themselves ($w_{2-4} \simeq 0.167$); and sc_3 with w_1 = 1 to minimize the structure's weight and w_{2-4} = 0 for the other objective functions, extracting the lightest solution from the Pareto front.

3 Geometrically nonlinear analysis

The geometrically nonlinear analysis contemplates the effects caused by the deformation and displacements of the structures. The primary objective of nonlinear analysis is to search for the equilibrium configuration of structures that are under the action of external loads [11]. As commented by Bonet [12], several methods combining load and displacement increments have been proposed to deal with nonlinear problems, but they have been replaced by arc-length methods, which compel the iterative solution to follow a certain route towards the equilibrium path. The family of techniques known as arc-length consists of controlling the length of the vector that connects a known point of the equilibrium trajectory to the desired unknown point, that is, the length of the arc that determines the correct trajectory.

In this paper, the cylindrical arc-length method, proposed by Crisfield [13], is applied to perform the geometrically nonlinear analysis of the truss dome. This analysis allows the definition of the structure's deformed configuration (final geometry after the application of loads), influencing the determination of the natural frequencies of vibration, and the critical load factor related to global stability, which are objective functions in the proposed MOSOP, as well as the calculation of nodal displacements, used as design constraints. The variable tangent stiffness matrix is calculated in each iteration according to the updated Lagrangian formulation, in which the equations are defined based on the equilibrium configuration of the previous load step. This process was realized through the program "NUMA-TF (Numerical Analysis of Trusses and Frames)", developed by Rangel [14]. The parameters of the arc-length procedure used in the program's simulation are: i- increment of load ratio in the predicted solution of first step = 0.01; ii- limit value of load ratio to stop analysis = 1; iii- maximum number of load steps to stop analysis = 5000; iv- maximum number of iterations in each step = 100; v- desired number of iterations in each step = 2; vi- tolerance to assume that equilibrium has been reached = 10^{-6}.

4 Formulation of the MOSOP and computational experiment

The truss under study is the 60-bar, 25-node shallow dome shown in Figure 1, also analyzed in Mai et al [11]. The design variables are the cross-sectional areas of the bars, divided in 7 groups as shown in Figure 1. The variables are discrete and chosen from the 19 options in the set S_{cm^2} = 0.50, 0.75, 1.00, ...4.25, 4.50, 4.75, and 5.00 cm^2. The aluminum bars have a specific mass of 2770 kg/m^3 and Young's modulus of 73 GPa. A vertical downward load is applied to node 1 in the z-direction, with the value F = 10000 N. The proposed MOSOP contains the four objective functions detailed in Section 2.1. Regarding the constraint, the displacement of the central node must not exceed $\pm$ 25 cm in the z direction. The application of the displacement constraint is based on Mai et al [11], in which this is the only type of constraint used in the optimization problems. The maximum allowed displacement is based on [11] and on experimental analyses performed by the authors. The MOSOP was evaluated through 10 independent runs of the DE-based algorithms presented in Section 2.2, each run with 50 generations of 20 individuals (1000 nfe). Since $W(\mathbf{x})$ is the weight of the truss, $f_1(\mathbf{x})$ is the first natural frequency of vibration, $\lambda_1(\mathbf{x})$ is the first critical load factor, $ncs(\mathbf{x})$ is the number of different cross-sectional areas for the bars, $u_1^z(\mathbf{x})$ is

the displacement of node 1 in the z-direction, $\mathbf{x}$ represents the design variables, and $\mathbf{x}^L$ and $\mathbf{x}^U$ indicate their lower and upper boundaries, this optimization problem can be written as follows:

MOSOP 1:

$$\begin{aligned} \min \quad & W(\mathbf{x}), \quad \max f_1(\mathbf{x}), \quad \max \lambda_1(\mathbf{x}), \quad \min \text{ncs}(\mathbf{x}), \\ s.t. \quad & |u_1^z(\mathbf{x})| \leq 25 \text{ cm} \\ & \mathbf{x}^L \leq \mathbf{x} \leq \mathbf{x}^U. \end{aligned} \tag{1}$$

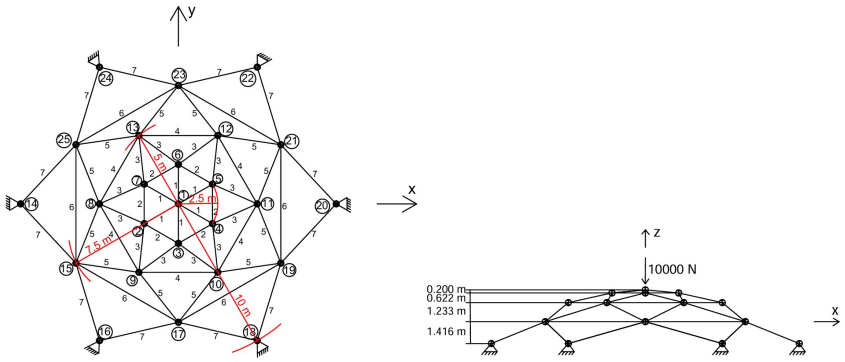


Figure 1. 60-bar truss dome.

5 Results of the MOSOP and extracted solutions

After formulating MOSOP 1, the problem was solved through the three algorithms presented in Section 2.2. The non-dominated solutions obtained by each meta-heuristic are presented in Figure 2, including the 3D graph with their weights, natural frequencies of vibration, and critical load factors, and also the variations of $W(\mathbf{x})$, $f_1(\mathbf{x})$, and $\lambda_1(\mathbf{x})$ with the number of different cross-sectional areas ($ncs(\mathbf{x})$). Figure 3a shows the unified PF for the 60-bar truss using parallel coordinates [15], while Figure 3b shows the same PF in 3D. The values of the objective functions are normalized to construct this PF and generate the parallel coordinates. This means that 1 represents the maximum value obtained and 0 the minimum value for each objective function. The results obtained by each algorithm are illustrated with different colors in Figures 2 and 3. The solutions extracted from the Pareto front using the MTD method are highlighted in these figures, following the pattern: green for MTD(sc_1), blue for MTD(sc_2), and magenta for MTD(sc_3), according to the weights of each scenario defined in Section 2.2.

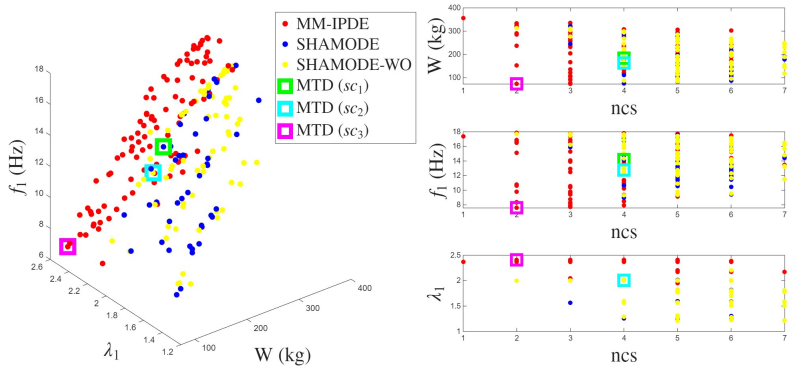
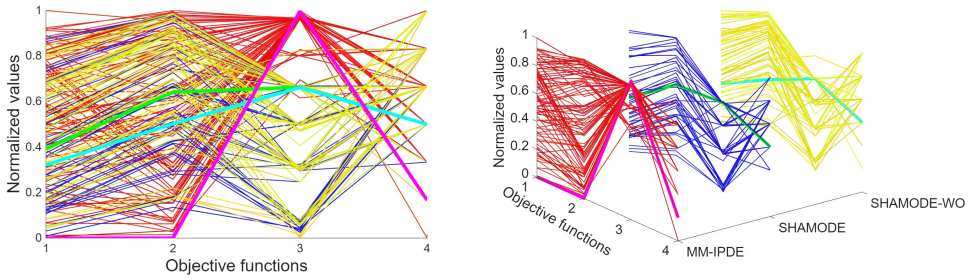


Figure 2. Pareto front and extracted solutions for the 60-bar truss dome - MOSOP 1.

Analyzing the non-dominated solutions obtained in Figures 2 and 3, it is possible to observe how the growth of the structure's weight causes increases in the first natural frequency of vibration. As for the critical load factor, the behavior isn't as clearly defined. The heavier trusses tend to present high values of $\lambda_1(\mathbf{x})$, but there are also lighter solutions with high critical load factors, for example, the one extracted for MTD(sc_3). It is also possible



(a) 2 dimensions (b) 3 dimensions

Figure 3. Normalized parallel coordinates PF for the 60-bar truss dome - MOSOP 1. The objective functions are 1: min $W(\mathbf{x})$, 2: max $f_1(\mathbf{x})$, 3: max $\lambda_1(\mathbf{x})$, 4: min $ncs(\mathbf{x})$.

to see a subtle tendency of diminishing the weight of the truss with a higher number of different cross-sectional areas, while the behaviours of $f_1(\mathbf{x})$ and $\lambda_1(\mathbf{x})$ don't show clear tendencies with the variation of $ncs(\mathbf{x})$.

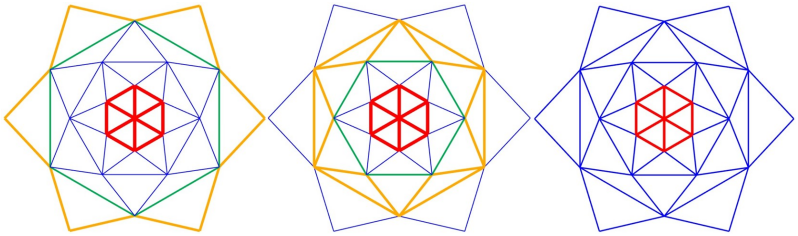
Table 1 provides a compilation of the solutions extracted with the three MTD scenarios. Table 1 also presents the cross-sectional areas of the bars, the axial stresses calculated for each group of bars (positive values for tension and negative values for compression), the DE-based algorithms that provided the solutions, and the values of the objective functions. Figure 4 illustrates the arrangement of the bars in the MTD solutions, with different colors for the distinct cross-sectional areas of each scenario. This data provides the designer with indications of the bars for constructing the structure to obtain the desired configuration and characteristics. Compared to the other scenarios, the solution MTD(sc_3) presents a much lighter structural configuration, maintaining a high value of $\lambda_1(\mathbf{x})$. This increased result for $\lambda_1(\mathbf{x})$ can be explained by the use of the largest cross-sectional area (5.00 cm^2) for the central bars (groups 1 and 2 of Table 1, colored in red in Figure 4c), while the low weight is a consequence of the smallest cross-sectional area (0.50 cm^2) defined for the peripheral bars (groups 3 to 7, represented in blue in Figure 4c). However, the value of $f_1(\mathbf{x})$ for this scenario is considerably lower than the ones obtained in the solutions MTD(sc_1) and MTD(sc_2). It can also be highlighted that the structure extracted for MTD(sc_3) uses only two different cross sections for the bars, countering the trend of diminishing the weight by increasing $ncs(\mathbf{x})$. In figures 4a and 4b, it is also possible to observe that the optimization process defined the largest cross sections for the central bars (groups 1 and 2), providing structural configurations with high indicators of frequency and stability, while meeting the displacement constraints.

Finally, Figure 5 shows the "Load x displacements" graphs for the MTD solutions of each scenario. It is possible to observe the nonlinear curves of the trusses throughout the application of the load at node 1. In these graphs, the applied load varies from 0 to 15 kN (a load higher than the 10 kN applied in the MOSOP), resulting in displacements larger than the 25 cm constraint, in order to illustrate the structure's nonlinear behaviour. The trusses indicated for MTD(sc_1) and MTD(sc_2) present very similar results. Otherwise, the lightest solution MTD(sc_3) presents the lowest load value and the greatest displacement at the first post-buckling point. Thus, the MTD(sc_3) structure presents the largest displacements for the central node of the dome.

Table 1. Design variables (dv), cross-sectional areas (cs), axial stresses in the i-th group of bars (σ_i), and objective functions of the MTD solutions extracted from the unified PF of the 60-bar truss dome - MOSOP 1.

	sc_1		sc_2		sc_3	
dv	cs (cm^2)	$\sigma_i(\mathbf{x})$ (MPa)	cs (cm^2)	$\sigma_i(\mathbf{x})$ (MPa)	cs (cm^2)	$\sigma_i(\mathbf{x})$ (MPa)
1	4.7500	-60.7272	4.7500	-60.7437	5.0000	-55.1710
2	4.7500	50.0641	4.7500	50.1155	5.0000	44.1966
3	1.5000	-28.8541	1.2500	-34.5188	0.5000	-93.4473
4	1.5000	38.2984	2.0000	28.6130	0.5000	127.4303
5	1.5000	-19.0882	2.7500	-10.3961	0.5000	-57.8083
6	2.0000	14.6803	2.7500	10.6323	0.5000	59.4516
7	4.0000	-7.8361	1.2500	-25.1603	0.5000	-63.1527
$W(\mathbf{x})$ (kg)	184.5192		164.2626		73.1101	
$f_1(\mathbf{x})$ (Hz)	14.1589		12.7310		7.5697	
$\lambda_1(\mathbf{x})$	2.0070		2.0054		2.4106	
$ncs(\mathbf{x})$	4		4		2	
Algorithm	SHAMODE		SHAMODE-WO		MM-IPDE	

Regarding the algorithms, MM-IPDE was the one that provided more non-dominated solutions (46.41% of the total amount of the Pareto front), followed by SHAMODE-WO (32.54%) and SHAMODE (21.05%). The



(a) MTD(sc_1). $ncs(\mathbf{x}) = 4$ (b) MTD(sc_2). $ncs(\mathbf{x}) = 4$ (c) MTD(sc_3). $ncs(\mathbf{x}) = 2$

Figure 4. Arrangement of the bars for the MTD solutions of the 60-bar truss dome - MOSOP 1.

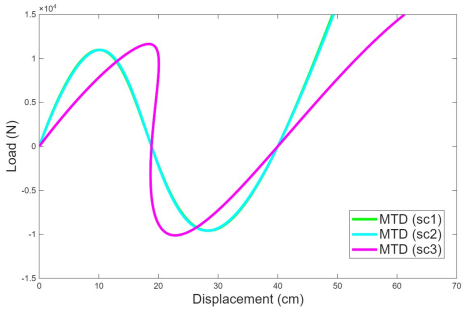


Figure 5. Load $\times$ displacements curves (node 1) for the MTD solutions of the 60-bar truss dome - MOSOP 1.

Hypervolume (HV) [16] was used as the performance indicator to analyze the efficiency of the meta-heuristics in solving MOSOP 1. Observing the relative HVs of the algorithms (HV_n, normalized by the HV of the total Pareto front, with all non-dominated solutions), the HV-metric indicated MM-IPDE as the best performer ($HV_n = 0.9576$), and then SHAMODE-WO ($HV_n = 0.6092$) and SHAMODE ($HV_n = 0.5285$). Regarding the computational costs for solving the MOSOP, MM-IPDE presented the highest average execution time per run (15 minutes and 23 seconds), slightly longer than the average time obtained for the runs of SHAMODE-WO (14 minutes and 52 seconds) and SHAMODE (13 minutes and 37 seconds).

6 Conclusions

The application of MOSOPs is an efficient method to find the desired configurations for a truss structure, with the characteristics, stability, and safety intended by the decision-maker. The MOSOPs provide the designer with a set of solutions that meet the constraints and reach the proposed objectives, allowing the DM to select those that best meet their preferences and intentions. Thus, these multi-objective problems provide a broad and diversified view of possible structural solutions, considering various demands and requirements, without the need to solve multiple single-objective problems individually. The chosen objective functions are very useful and important for obtaining lighter and more economical solutions while maintaining the structure's safety and usability. The results obtained for the proposed MOSOP clearly show that minimizing the weight is a conflicting objective concerning maximizing the first natural frequency of vibration. As for the number of different cross-sections, a slight decay of $W(\mathbf{x})$ is observed when increasing $ncs(\mathbf{x})$, while $f_1(\mathbf{x})$ and $\lambda_1(\mathbf{x})$ don't show clear trends.

The MTD method proved to be very efficient in finding structures that met the DM's criteria according to the importance (weight) attributed to each objective function. Analyzing the extracted MTD solutions, it can be observed that the MTD(sc_3) structure was able to present a much lighter configuration with a higher value of $\lambda_1(\mathbf{x})$, despite the lower frequency of vibration and larger displacements compared to the other MTD scenarios. The low weight and high stability of MTD(sc_3) can be attributed to a favorable arrangement of the bars, with a layout that places the largest cross-sectional areas in the central region (where the load is applied and the constraint is analyzed) and the smallest cross sections at the peripheral bars of the truss. Observing the "Load x displacements" graphs for these solutions, it's possible to note the intense nonlinear behavior of the analyzed dome. This behavior emphasizes the importance of the geometrically nonlinear analysis to define the deformed configuration in this type of structure, calculating the objective functions and constraints with greater accuracy, despite the higher computational costs, when compared to linear evaluations. Regarding the algorithms, the MM-IPDE presented the

best performance, providing more non-dominated solutions and the best hypervolume, followed by SHAMODE-WO and SHAMODE, despite having an average execution time slightly higher than the other meta-heuristics.

Therefore, the paper fulfilled the objectives of proposing and solving a new MOSOP, including important objective functions and the geometrically nonlinear analysis of the shallow dome. Future work is expected to propose new MOSOPs that consider the inclusion of more objective functions (many-objective optimization problems), applying these problems to structures of different types and complexities. Finally, machine learning algorithms will be applied to minimize the high computational costs required to perform the nonlinear analysis and evaluate the objective functions and constraints.

Acknowledgements. The authors wish to thank the Graduate Program in Computational Modeling (UFJF), the Federal University of Juiz de Fora, the Federal University of São João del-Rei, the Federal Center for Technological Education of Minas Gerais, FAPEMIG (TEC PPM 174-18), CAPES, and CNPq (Grants 308105/2021-4 and 303221/2022-4) for their support.

Authorship statement. The authors hereby confirm that they are the sole liable persons responsible for the authorship of this work, and that all material that has been herein included as part of the present paper is either the property (and authorship) of the authors, or has the permission of the owners to be included here.

References

[1] J. P. G. Carvalho, A. C. C. Lemonge, P. H. Hallak, Érica C. R. Carvalho, and H. S. Bernardino. Truss optimization with multiple frequency constraints and automatic member grouping. *Structural and Multidisciplinary Optimization*, vol. 57, pp. 547–577, 2017.

[2] J. Carvalho, E. Carvalho, D. Vargas, P. Hallak, B. Lima, and A. Lemonge. Multi-objective optimum design of truss structures using differential evolution algorithms. *Computers & Structures*, vol. 252, pp. 106544, 2021.

[3] J. C. Motta. Otimização espacial multi-objetivo de pórticos espaciais em aço com variáveis de projeto não usuais. Master's thesis, Programa de Pós-Graduação em Engenharia Civil, Faculdade de Engenharia, Universidade Federal de Juiz de Fora, 2022.

[4] J. M. P. Vieira, J. P. G. Carvalho, D. E. C. Vargas, E. C. R. Carvalho, P. H. Hallak, and A. C. C. Lemonge. Many-objective truss structural optimization considering dynamic and stability behaviors. *Dynamics*, vol. 5, n. 1, 2025.

[5] R. Storn and K. Price. Differential evolution a simple and efficient adaptive scheme for global optimization over continuous spaces. Tech. Rep. 95-012, Univ. of California, Berkeley, CA, 1995.

[6] N. Panagant, S. Bureerat, and K. Tai. A novel self-adaptive hybrid multi-objective meta-heuristic for reliability design of trusses with simultaneous topology, shape and sizing optimisation design variables. *Structural and Multidisciplinary Optimization*, vol. 60, n. 5, pp. 1937–1955, 2019.

[7] K. Wansasueb, N. Pholdee, N. Panagant, and S. Bureerat. Multiobjective meta-heuristic with iterative parameter distribution estimation for aeroelastic design of an aircraft wing. *Engineering with Computers*, vol. 38, pp. 1–19, 2020.

[8] K. Deb, A. Pratap, S. Agarwal, and T. Meyarivan. A fast and elitist multiobjective genetic algorithm: NSGA-ii. *IEEE Transactions on Evolutionary Computation*, vol. 6, n. 2, pp. 182–197, 2002.

[9] R. Parreiras and J. Vasconcelos. Decision making in multiobjective optimization aided by the multicriteria tournament decision method. *Nonlinear Analysis: Theory, Methods & Applications*, vol. 71, n. 12, pp. e191–e198, 2009.

[10] A. Lemonge, J. Carvalho, P. Hallak, and D. Vargas. Multi-objective truss structural optimization considering natural frequencies of vibration and global stability. *Expert Systems with Applications*, vol. 165, pp. 113777, 2021.

[11] H. T. Mai, J. Kang, and J. Lee. A machine learning-based surrogate model for optimization of truss structures with geometrically nonlinear behavior. *Finite Elements in Analysis and Design*, vol. 196, pp. 103572, 2021.

[12] J. Bonet and R. Wood. *Nonlinear Continuum Mechanics for Finite Element Analysis*. Cambridge University Press, 2 edition, 2008.

[13] M. Crisfield. *Nonlinear finite element analysis of solids and structures*. John Wiley & Sons, 2003.

[14] R. L. Rangel. Educational tool for structural analysis of plane frame models with geometric nonlinearity. Master's thesis, Programa de Pós-graduação em Engenharia Civil, PUC-Rio. In Portuguese, 2019.

[15] M. Li, L. Zhen, and X. Yao. How to read many-objective solution sets in parallel coordinates [educational forum]. *IEEE Computational Intelligence Magazine*, vol. 12, n. 4, pp. 88–100, 2017.

[16] E. Zitzler and L. Thiele. Multiobjective evolutionary algorithms: a comparative case study and the strength pareto approach. *IEEE Transactions on Evolutionary Computation*, vol. 3, n. 4, pp. 257–271, 1999.